Composites: Part A 68 (2015) 193–201

Contents lists available at ScienceDirect

Composites: Part A

journal homepage: www.elsevier.com/locate/compositesa

Crystallization, mechanical performance and hydrolytic degradation of poly(butylene succinate)/graphene oxide nanocomposites obtained via in situ polymerization

Tian-Xiang Jin [a], Chuan Liu [a], Mi Zhou [a], Song-gang Chai [b], Feng Chen [a,*], Qiang Fu [a,*]

[a] College of Polymer Science and Engineering, Sichuan University, State Key Laboratory of Polymer Materials Engineering, Chengdu 610065, China
[b] National Engineering Research Center of Electronic Circuits Base Materials, Dongguan 523039, China

ARTICLE INFO

Article history:
Received 12 July 2014
Received in revised form 29 September 2014
Accepted 30 September 2014
Available online 13 October 2014

Keywords:
A. Polymer–matrix composites (PMCs)
B. Interface/interphase
B. Mechanical properties
E. Melt-spinning

ABSTRACT

Poly(butylene succinate) (PBS)/graphene oxide (GO) nanocomposites were fabricated via in situ polymerization with very low GO content (from 0.03 to 0.5 wt%). The microstructures of the nanocomposites were characterized with Raman spectroscopy, fourier transform infrared spectroscopy (FTIR), thermogravimetric analysis (TGA), sedimentation experiments and atomic force microscopy (AFM). The results showed that PBS chains have been successfully grafted onto GO sheets during in-situ polymerization, accompanied by the thermo-reduction from GO to graphene. The grafted GO displayed a great nucleating effect on PBS crystallization, resulting in largely improved crystallization temperature and decreased spherules size. A simultaneous enhancement in tensile strength and elongation was achieved for PBS/GO nanocomposites fiber. Meanwhile, increase in hydrolytic degradation rate was also observed for these nanohybrids. Our result indicates that using very low content GO is a simple way to achieve good dispersion yet with remarkable property enhancement for polymer/GO nanocomposites.

1. Introduction

Poly(butylene succinate) (PBS) is a new type of biodegradable material. As an eco-friendly polyester, PBS can be widely applied in agriculture, forestry, civil engineering, and other fields [1,2]. However, some properties of PBS, such as mechanical properties and degradation rate, are often not sufficient for various end-use applications.

The addition of nanoparticles into polymeric matrix is an effective way to improve the performance of polymers [3–6]. Graphene has been highlighted in fabricating polymer nanocomposites in recent years because of its unique structure and properties. Graphene sheet has high young's modulus, fracture strength [7], thermal conductivity (~5000 Wm^{-1} K^{-1}) [8], and good electrical conductivity [9]. Thus, the preparation of PBS/graphene nanocomposites is a very promising way to improve the properties of PBS. However, graphene sheets have a strong tendency to agglomerate due to van der waals force which severely limits the performance of its composites. Three methods have been used to disperse graphene into polymer: melt blending [10,11], solvent blending [12] and in-situ polymerization [13]. The melt blending causes poor dispersion while the in-situ polymerization and solvent blending usually result in good dispersion. However, the solvent blending requires large amounts of organic solvent which is poisonous and harmful to the environment. Therefore, in-situ polymerization technique is a particularly attractive way to solve this problem. Moreover, by using the functional groups on the surface of graphene oxide (GO), one can make GO well dispersed in monomer first and then GO will be thermally-reduced to graphene simultaneously under high temperature during polymerization. The preparation of poly(butylene succinate)/graphene oxide composites was reported by Xiao [14]. They found that tensile stress of the composite was 43% higher than those of pure PBS when GO content reaches 3 wt%. The enhancement is not so obvious comparing with other polymer/GO nanocomposites reported. In addition, since the reactive groups on GO sheet could disrupt the stoichiometric balance between hydroxyl groups and carboxylic acids in polyester reaction system [15], the molecular weight of polymer matrix is usually very much decreased. Thus, the elongation at break of these composites in their work was decreased dramatically after GO was added. Besides, other molecular weight-related properties such as crystallization properties and degradation also cannot be investigated and compared because of the large difference in the molecular weight between pure PBS and the composites.

* Corresponding authors. Tel.: +86 28 85460690 (F. Chen), +86 28 85461795 (Q. Fu).
E-mail addresses: fengchen@scu.edu.cn (F. Chen), qiangfu@scu.edu.cn (Q. Fu).

http://dx.doi.org/10.1016/j.compositesa.2014.09.025
1359-835X/

In this work, PBS/GO composites is prepared via in-situ melt polymerization and simultaneous thermo-reduction of GO. The difference of our work from the reported work is that: the filler contents were controlled to be very small amount (less than 0.5 wt%). In this way, GO could have a better dispersion, and more importantly, the effect of GO on the polymerization can be largely decreased. By controlling the polymerization times, we have successfully obtained PBS/GO nanocomposites with similar matrix molecular weight. Then, the dispersion and interaction between the filler and PBS was studied, and the influence of filler on crystallization, mechanical performance and hydrolytic degradation were investigated. Our results demonstrate that using very low content GO is a simple way to achieve good dispersion, similar matrix molecular weight, yet remarkable property enhancement in PBS/GO nanocomposites.

2. Experiment

2.1. Materials

Succinic acid (SA) was supplied by Kemiou Chemical Reagent Corporation (Tianjin, China), while 1,4-butanediol(BD), tetrabutyl titanium and triphenyl phosphate(TPP) were purchased from Kelong Chemical Corporation (Chengdu, China). All chemicals were analytical grade and used without any purification.

2.2. Sample preparation

A certain amount of GO water solution, which was prepared by Hummers' method [13], was firstly dispersed in 1,4-butanediol with vigorous agitation and ultrasonic treatment for 30 min at room temperature. Then, water in the solution was removed by distillation at 60 °C in vacuum. After cooling to room temperature, GO solution was added into a home-made autoclave together with quantitative amount of succinic acid and was charged into a home-made reactor together with tetrabutyl titanium and TPP (tetrabutyl titanium as catalyst, TPP as stabilizer). With stirring, the reaction mixture was heated at 180 °C for 2.3 h under nitrogen atmosphere. Then, temperature was progressively increased to 230 °C, and pressure was reduced to 65 Pa for condensation polymerization. To control condensation time, the electric current used to drive the stirring rod was set to a designed value. As the stirring electric current value is influenced by the molecular weight and GO content of the sample, therefore, we can carefully adjust the electric current value to make sure the samples with different GO content have similar molecular weights. After polymerization, the product was extruded into cold water from the reactor by compressed nitrogen, and cut into pellets. In our experiments, other samples containing 0.03 wt%, 0.05 wt%, 0.1 wt%, 0.3 wt% and 0.5 wt% GO were synthesized with the same procedure and were labeled as PBSG-003, PBSG-005, PBSG-010, PBSG-030, and PBSG-050, respectively. The products were chopped into small pieces and dipped in distilled water for 5 h to remove low-molecular-weight oligomers and monomer completely. After being dried in vacuum at 50 °C for 24 h, the products were melt-spun into fibers at 140 °C using a set of melt-spun devices adapted to the piston-mode Rosand RH70 (Malvern, Bohlin Instruments) capillary rheometer. The capillary has a die diameter of 1.0 mm and a length-to-diameter ratio of 16. The extruded-composite fibers were air-cooled and were enwound on a steadily rotating roll. The enwound speeds were 200 m min^{-1} and the fiber diameter was 55 ± 3 micrometer (measured by a micrometer).

In order to investigate the interaction between PBS and GO surface, successive centrifugation/redissolution cycles were employed to separate GO from physically absorbed polymer. The centrifugation and dissolution procedure is described as follows: the composites were dissolved in dichloromethane and then the suspension was centrifuged at 11,000 rpm for 30 min to make GO completely precipitated. The supernatant was filtered to remove residual GO and used for molecular weight test while the obtained sediment was dissolved in the dichloromethane again, and ultrasonic treatment for 20 min to remove physically absorbed PBS from GO surface, then separated by centrifugation again. This centrifugation and dissolution procedure was performed repeatedly for 7 times. The resulting solid materials were freeze-dried to keep loosely stacked sheets. The final obtained sheet is called IS-G.

2.3. Characterization

The intrinsic viscosity was measured by an ubbelohde viscometer at a concentration of 0.4 g/dL in chloroform at 25 °C. Intrinsic viscosity was calculated after the Solomon–Ciuta equation [16]:

$$[\eta] = [2\{t/t_0 - \ln(t/t_0) - 1\}]^{1/2} \Big/ c \quad (1)$$

The viscosity-average molecular weight (M_η) was calculated from

Mark–Houwink equation [14]:

$$\eta = K[M_\eta]^\alpha \text{ (where } K = 1.71 \times 10^{-4}, \text{ and } \alpha = 0.79) \quad (2)$$

The FTIR spectra were recorded between 400 cm^{-1} and 4000 cm^{-1} on a Nicolet-560 infrared spectrometer. The sample was coated on a KBr plate.

The thermal stability was studied by thermal gravimetric analysis (TGA) test, conducted at WRT-2P (Shanghai Scale Factory), from 30 °C to 700 °C in nitrogen atmosphere with heating of 10 °C min^{-1}.

A micro-Raman spectrophotometer (Renishaw) was used to characterize GO, and IS-G. The laser was excited by the 136 M Het resource with a wavelength of 514.5 nm.

The melting behavior of prepared PBS/GO nanocomposites was studied by differential scanning calorimetry (DSC) with a Perkin Elmer DSC Pyris-1. Every sample (about 4.5–5.5 mg) was subjected to heating from room temperature to 150 °C as quick as possible, held at 150 °C for 3 min to eliminate the thermal history, and cooled down to 30 °C at scan rate of 10 °C/min. Then the same sample was heated again to 150 °C at a rate of 10 °C/min.

The crystallinity (X_c) of the samples were determined by a wide angle X-ray diffractometer (Philips X'Pert pro MPD) in the 2θ range of 5–40°(5°/min) according to the following equation:

$$X_c = \frac{\sum A_{cryst}}{\sum A_{cryst} + \sum A_{amorp}} \times 100\% \quad (3)$$

where A_{cryst} and A_{amorp} represent for the integral intensities of crystalline and amorphous regions, respectively. The measurement was performed using a conventional Cu Kα X-ray (λ = 0.154 nm, reflection mode) tube at a voltage of 40 kv and a filament current of 40 mA.

The crystal morphology was studied on a polarized optical microscope equipped with a hot stage. Samples were first heated at 150 °C for 3 min to erase the thermal history, then cooled to 85 °C at 100 °C/min for isothermal crystallization.

For scanning electronic microscopy (SEM) investigation, PBS composites were cryo-fractured in liquid nitrogen and investigated on an Inspect SEM instrument (FEI) with an acceleration voltage of 20 kV.

The mechanical properties of fibers were measured with a tensile strength tester (LLY-06E, Laizhou, China). The initial length is 20 mm; drawing speed is 20 mm/min. At least five samples were

used for each measurement and the results were averaged to obtain a mean value.

Two-dimensional wide-angle X-ray scattering (2D-WAXS) experiments were conducted on a Bruker Discover 8 diffractometer. The wavelength of the monochromated X-ray from Cu radiation was 0.154 nm, and the sample-to-detector distance was 273 mm. The samples were placed with the orientation (drawing direction) perpendicular to the beams. Azimuthal scans (0–360°) 2D-WAXS were made for the test samples at a scan speed of 1.0°/min. The orientation degree of crystal planes could be calculated by the orientation parameter f from the following equation:

$$f_H(\cos\varphi) = \frac{3\langle\cos^2\varphi\rangle - 1}{2} \tag{4}$$

$$\langle\cos^2\varphi\rangle = \frac{\int_0^{\frac{\pi}{2}} I(\varphi)\sin\varphi\cos^2\varphi d\varphi}{\int_0^{\frac{\pi}{2}} I(\varphi)\sin\varphi d\varphi} \tag{5}$$

where φ is the angel between the normal of a given (hkl) crystal plane and the drawing direction and I is the intensity. A perfectly perpendicular orientation gives f = 1.0. An un-oriented sample gives f = 0.

The dimension of the hydrolytic degradation samples molded by hot pressing was 30 × 9 × 0.5 mm. Each specimen was dipped in a flask containing 100 ml NaOH solution (2 mol/L). Then, these flasks were put in a water bath at 40 °C. After a fixed period of time these samples were picked out and washed with distilled water to remove any traces of NaOH solution and then dried to a constant weight in vacuum oven at 50 °C.

3. Results and discussion

3.1. Characterization of interaction between PBS and GO

In order to improve the mechanical properties of PBS composites, strong interaction between fillers and polymer matrix is needed for effective transfer of stress and load distribution throughout the interface. It is well known that the chemical bonding between the fillers and polymer matrix is favorable for the improvement of interfacial interactions in polymer/filler composites [13,15,17]. In this work, GO was introduced into PBS matrix via in-situ polymerization, which allowed PBS chains to be linked on GO sheets, forming novel polymer grafting interface structures (Scheme 1). In order to further investigate the possible grafting of PBS chain on the surface of GO, we characterized the fillers which were separated from the composites, named as "IS-G".

The FTIR spectra of GO, IS-G and PBS are shown in Fig. 1. There are a number of peaks in the FTIR spectra of GO. The characteristic peaks are those in the region of 1390 cm^{-1}, 1063 cm^{-1}, 1254 cm^{-1}, 1102 cm^{-1} for O—H bending vibrations, C—OH stretching vibrations, C—O stretching vibrations from carboxylic groups, and C—O stretching vibrations, respectively.

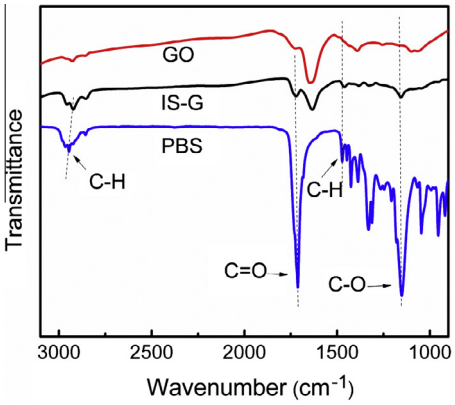

Fig. 1. FTIR spectra of GO, IS-G and PBS. (For interpretation of the references to colour in this figure legend, the reader is referred to the web version of this article.)

In the absorption spectrum of IS-G, all the characteristic absorption bands of oxide groups mentioned above are decreased, indicating that GO has been partially reduced. The appearance of a peak at 2924 cm^{-1}, 1712 cm^{-1}, 1472 cm^{-1} and 1155 cm^{-1}, which corresponds to the stretching vibrations of C—H, —C=O stretching vibration, C—H bending vibration and C—O stretching vibration in the ester group of PBS, indicates that GO is grafted by PBS chains [18].

The grafting of PBS chains onto GO surface can be further proved by the dispersion of IS-G in dichloromethane solvent. As shown in Fig. 2(a), the pendent PBS chains on IS-G platelets offer strong interaction with dichloromethane, resulting in a homogeneous dispersion of IS-G sheets in dichloromethane, while aggregation of GO sheets is observed in dichloromethane.

Fig. 2(b) and (c) shows the tapping mode AFM images of GO and IS-G sheets. After grafting PBS on two sides of GO sheets, the thickness of IS-G sheets increases from 0.8 nm to 4 nm, which primarily originated from the contribution of grafting PBS. Interestingly, such PBS-grafted GO nanosheets show a novel kind of 2D macro-molecular brushes, which can be applied as building blocks for the facile fabrication of large-area surface brushes used in surface engineering and nanotechnology [19].

The amount of PBS chains grafted on GO sheets can be estimated by TGA measurement. The weight loss curves for GO, neat PBS and IS-G are presented in Fig. 3.

It is found that neat PBS is decomposed at 400 °C which is consistent with other literature [20]. The main weight loss of GO is from 150 °C to 250 °C, due to the removal of some oxygen-containing functional groups bonded to GO sheets [21]. The decomposition temperature of IS-G is slightly lower than neat PBS, which may be caused by the further thermal reduction of GO. From the weight

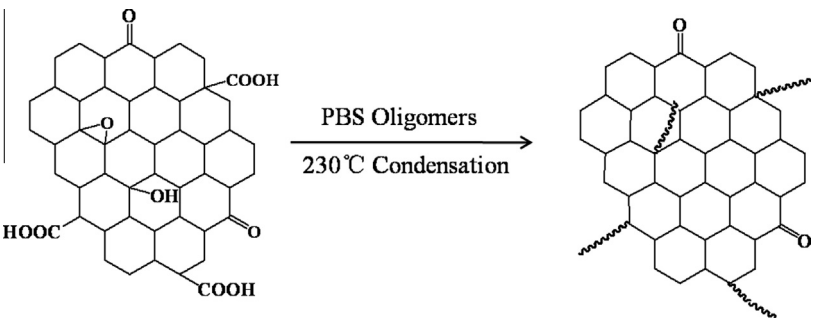

Scheme 1. Synthesis of PBSG composites by in situ polymerization.

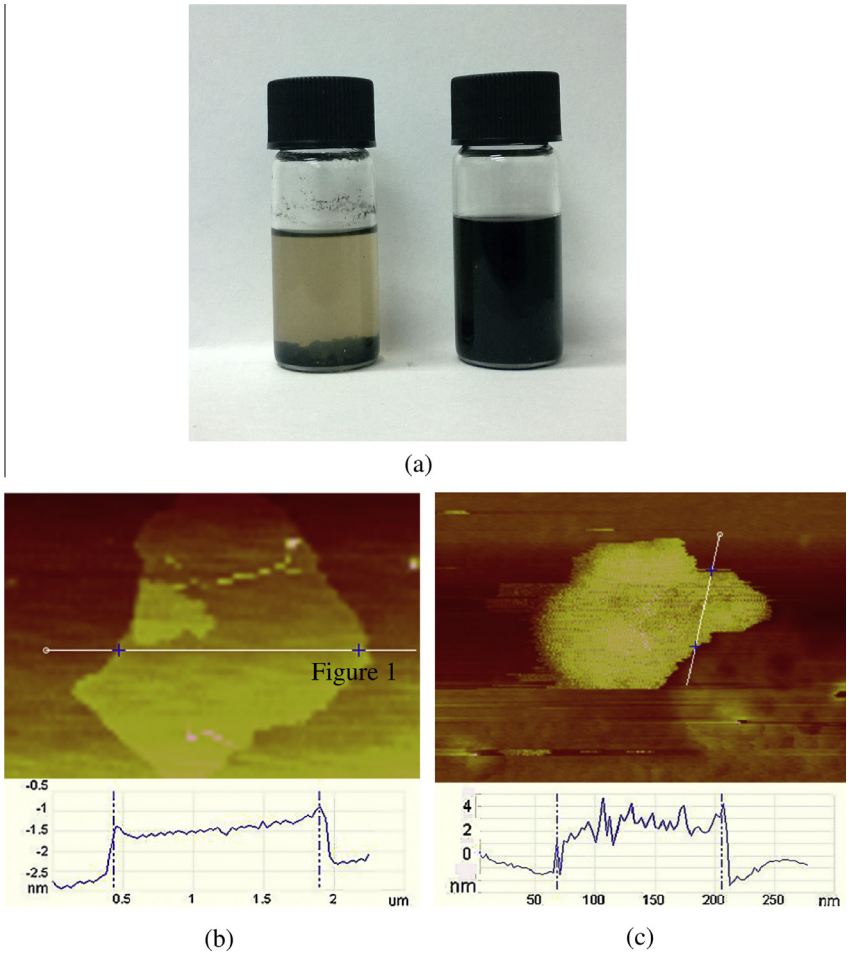

Fig. 2. (a) GO in dichloromethane (left), IS-G in dichloromethane (right), AFM image of GO (b) and IS-G (c). (For interpretation of the references to colour in this figure legend, the reader is referred to the web version of this article.)

loss of IS-G, the mass fraction of PBS chains grafted on GO sheets can be calculated to be around 81%.

Since the polymerization of PBS was carried out at 230 °C, one also expects an in-situ thermal reduction of GO during polymerization [22]. Thus, Raman spectroscopy was employed to evaluate the thermal reduction of GO as shown in Fig. 4.

The D band and G band are attributed to the first-order scattering of the E2g vibration mode in graphite sheet and structure defects, respectively. GO exhibits one band at 1609.10 cm^{-1} (G band) and the other band at 1350.9 cm^{-1} (D band). In the Raman spectra of IS-G, the G band red-shifts to 1597.6 cm^{-1}, which is close to the value of graphite, indicating a certain degree reduction of GO [23,24].

3.2. Characterization of the PBS and PBS/GO composites

3.2.1. The intrinsic viscosity of PBS and PBS/GO composites

As well known, both filler and polymer matrix can influence the properties of composites [25]. If we want to explore the role of

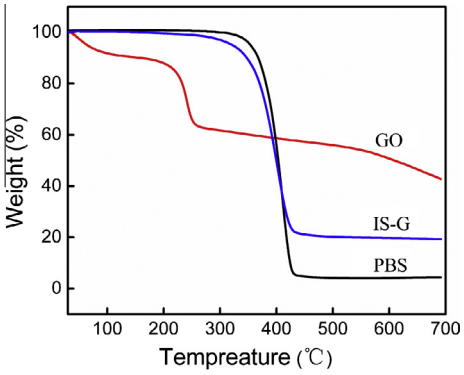

Fig. 3. TGA curves of GO, IS-G and PBS. (For interpretation of the references to colour in this figure legend, the reader is referred to the web version of this article.)

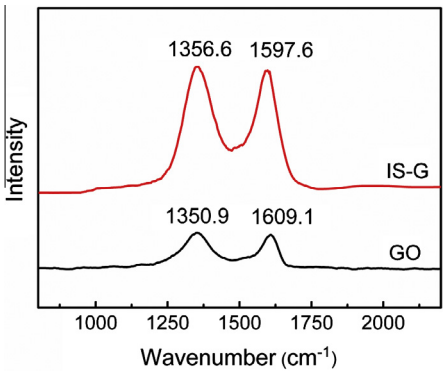

Fig. 4. Raman spectra of GO and IS-G. (For interpretation of the references to colour in this figure legend, the reader is referred to the web version of this article.)

filler in the composites fabricated by in-situ polymerization, the molecular weight must be more or less the same in all samples. Thus the molecular weight of PBS was measured via intrinsic viscosity for all the composites as well as the pure PBS sample, and the result is listed in Table 1.

As shown in Table 1, the intrinsic viscosities of all samples are in the range 1.053–1.103. The viscosity-average molecular weights (M_η) calculated from Mark–Houwink equation is in the range of 62,600–66,200. For these nanocomposites with different GO contents, the MW of PBS is almost constant.

3.2.2. Crystallization behavior and crystal morphology

As a semicrystalline polymer, the crystallization behavior of PBS has important influence on its performance. The melt-crystallization behavior was investigated by DSC measurements.

Fig. 5(a) shows DSC cooling scan thermogram of PBS and its composites. Neat PBS crystallizes in a broad crystallization temperature range with a crystallization peak appearing at 60 °C. After adding 0.03 wt% of GO, the crystallization temperature (T_c) of PBS increases to 65 °C. As the content of GO further increasing, the T_c could reach 73 °C and the temperature range became narrow. It is indicated that these GO platelets in PBS matrix has nucleating effect on the crystallization of PBS. For melting curve, the melting point of PBS in composites is increased from 103 °C to 109 °C because of the improvement in crystallization temperature. Furthermore, there are two melting peaks melting curves for all samples. Double melting behavior, has been observed for many semicrystalline polymers, such as poly(butylene terephthalate) (PBT) [26], poly(ethylene terephthalate) (PET) [27], nylon 6 [28] and Poly(L-lactic acid) [29]. The appearance of double melting peaks originated from melting and recrystallization process of crystallites with low thermal stability [30]. A minor exothermal peak also can be observed in the heating curve of these samples and appeared just prior to melting peak. Two possibilities were considered to explain the origin of this crystallization exotherm. One possibility is that it was the cold crystallization of PBS chains which did not have enough time to crystallize during cooling. However, cold crystallization usually can be observed in polymers which have relatively slow crystallization rate and high glass-transition temperature. During the rapid cooling or quenching process, these polymer cannot fully crystallize. For PBS, it has relative fast crystallization rates and its glass-transition temperature is relatively low (around −30 °C). Besides, the cooling rate in our experiment is slow (10 °C/min). Therefore, the cold crystallization phenomenon in this test should be not obvious. It should be also noted that the crystallization temperature gradually increases with increasing GO content. This phenomenon also cannot be explain by cold crystallization, as the cold crystallization temperature usually decreases because of the heterogeneous nucleation effect of GO. The other possibility is that the minor crystallization exotherm was the melt-recrystallization of crystals with low thermal stability [31]. After adding GO, the crystallization temperature in the cooling curve is increased. The structure of crystal formed in higher temperature is more perfect and the thermal stability is also higher. Therefore, the crystal will melt-recrystallize at a higher temperature as GO content increases. From the above, we consider it is the melt-recrystallization of the unstable crystals formed during heating process. In order to avoid the influence of cold crystallization and melt-recrystallization on the crystallinity of these samples, we used DSC and WAXD to investigate the crystallinity (Table 1). The DSC and WAXD results corroborate each other and both the results show that the crystallinity is not changed obviously after adding GO.

The spherulite growth morphology of PBS and the composites was observed using POM. Showing as an example, the crystal morphologies of PBS and PBS/GO nanocomposites with GO content of 0.03 and 0.5 wt% isothermal crystallized at 85 °C are shown in Fig. 6. The number of spherulites in PBS increases evidently after

Table 1
Intrinsic viscosity and molecular weight of PBS and its composites.

Sample	PBS	PBSG-001	PBSG-003	PBSG-010	PBSG-030	PBSG-050
[η](dL/g)	1.062	1.056	1.103	1.095	1.089	1.053
M_η	63,300	62,900	66,200	65,800	65,300	62,600
X_c[a] (%)	48.0	50.4	48.7	45.3	46.6	45.9
X_c[b] (%)	51.4	53.2	50.7	49.5	50.2	48.0

[a] Determined by DSC.
[b] Determined by WAXD.

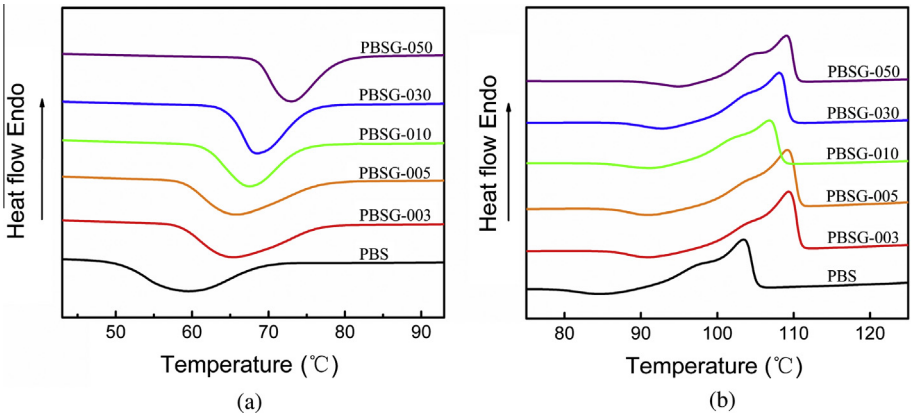

Fig. 5. DSC curves in the cooling (a) and heating and (b) process of PBS and its composites. (For interpretation of the references to colour in this figure legend, the reader is referred to the web version of this article.)

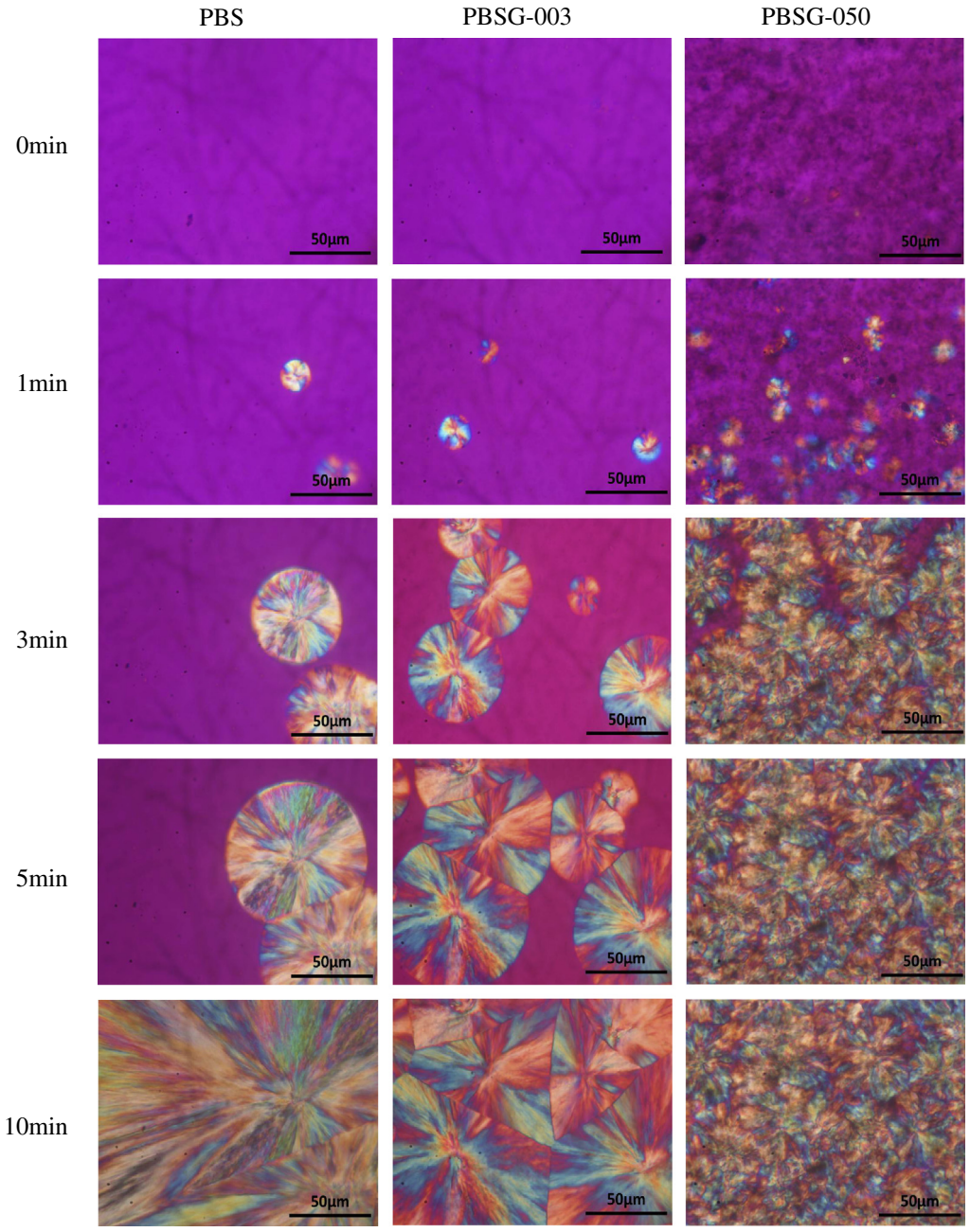

Fig. 6. POM micrographs of spherulites in PBS, PBSG-003 and PBSG-050 composites, after isothermal crystallization at 85 °C for 1, 3, 5, and 10 min. (For interpretation of the references to colour in this figure legend, the reader is referred to the web version of this article.)

adding a very small amount of GO. The size of spherulite is decreased from hundreds of micrometer for pure PBS to tens of micrometer for PBS/GO containing 0.5 wt% of GO. This result again suggests that GO serves as an effective nucleating agent for the crystallization of PBS.

3.2.3. Hydrolytic degradation

The hydrolytic degradation performance is one of the most important properties for biodegradable polymer. The degradation behaviors of aliphatic polyesters can be affected by many factors, such as pH, temperature, crystallinity, molecular weight and crystal morphology [32]. In this work, the same environmental conditions (pH and temperature) and samples with similar molecular weights were used to study the hydrolytic degradation of these composites. Fig. 7 shows the weight loss of PBS samples at different filler loadings during hydrolytic degradation. The weight loss data of sample with GO content more than 0.1 wt% are not shown here, because their degradation rate is too fast to keep their original shape during test. The degradation rates of neat PBS and the nanocomposites are obtained from the slopes of these hydrolytic degradation curves [33], and the slopes are listed in Table 1.

It can be observed that the hydrolytic accelerating effect of filler is obvious. For neat PBS, the hydrolytic degradation rate is around 0.252%/h; however, it increase to 0.726%/h when only 0.03 wt% GO is added into PBS matrix. The degradation rates can reach 2.08%/h which is eight times faster than the degradation rate of neat PBS with increasing GO loading to only 0.1 wt%. It is obvious that the nanocomposites degrade faster than neat PBS and the degradation rate increases with increasing GO content, and an order of magnitude increase of hydrolytic degradation rate can be achieved for the

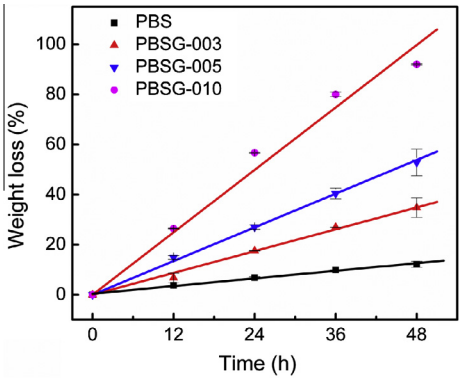

Fig. 7. Variation of weight loss with hydrolytic degradation time for neat PLLA and its composites. (For interpretation of the references to colour in this figure legend, the reader is referred to the web version of this article.)

nanohybrids with 0.1 wt% GO content, indicating the loading of GO significantly accelerates the hydrolytic degradation of PBS in the nanocomposites. For example, only 50 h is needed for completely degradation of PBS by adding only 0.1 wt% of GO. Since the crystallinity of all the samples is very similar, suggesting that crystallinity is not a factor influencing the hydrolytic degradation. Two possible reasons may be suggested for the improved hydrolysis rate of PBS composites. One reason is that the presence of GO can create more defects and gaps between filler and matrix which makes water molecules to penetrate more easily into the material to trigger degradation [34]. The other reason may be due to the well dispersion of GO which decreases the size of spherulite effectively and the spherulitic boundaries become loose. It is known that hydrolytic degradation proceeds faster in the amorphous region between the spherulitic than in the crystalline region [35]. Therefore, this crystal morphology with relatively smaller spherulitic may allow the water molecules diffuse easily into the interior of polymers through spherulitic boundaries [36,37].

3.2.4. The mechanical properties of PBS and its composites

The mechanical performance is important for further application of PBS. In order to strengthen the enhancement effect of the filler, the composites were melting spun into fibers and the mechanical properties are compared, this is shown in Fig. 8.

For oriented PBS fiber, the tensile strength is about 135 MPa, a maximum of 55% increase in tensile strength is observed for the composite sample containing only 0.05 wt% of GO sheets, and the tensile strength reaches 210 MPa. Then, a decrease in tensile strength is observed with further increasing GO content. Moreover, the elongation at break also can be improved from 280% for PBS to 610% for composite sample containing only 0.1 wt% of GO sheets. Such mechanical improvements could be attributed to the efficient load transfer between GO sheet and the PBS matrix. However, as the content of the GO further is increases beyond 0.1 wt%, the

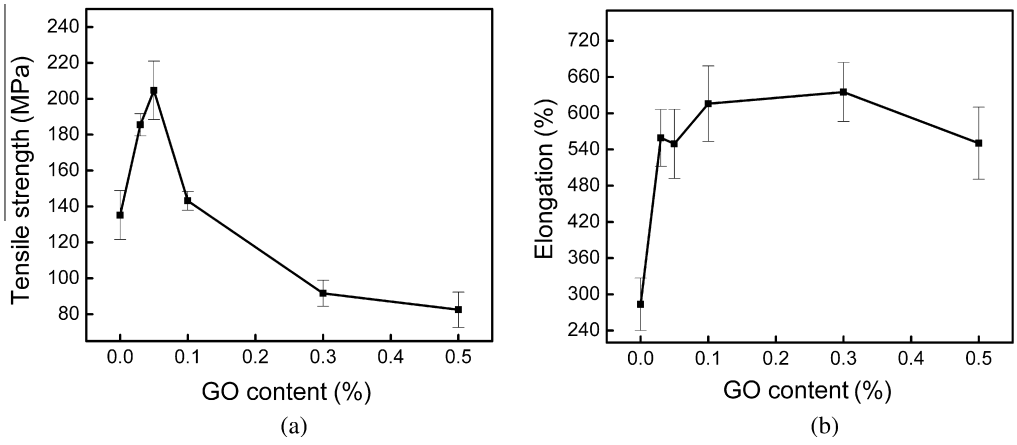

Fig. 8. Mechanical properties of neat PBS and its composites.

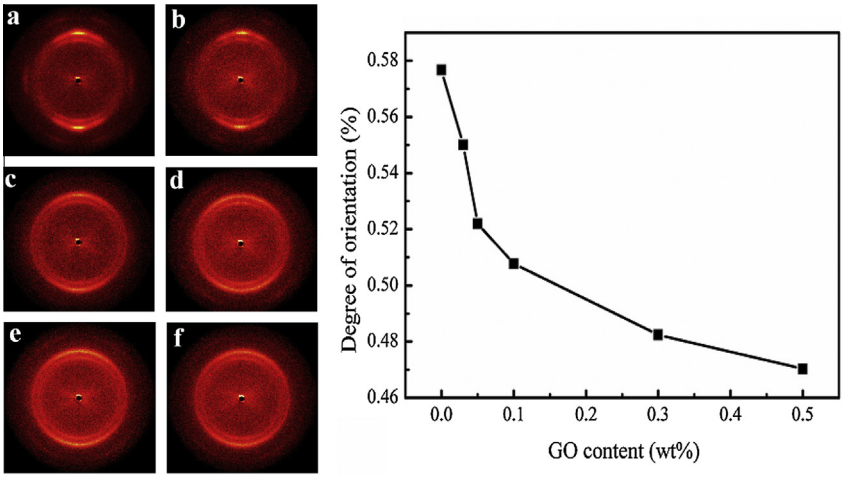

Fig. 9. 2D-WAXS patterns of composite fibers (a) neat PBS, (b) PBSG-003, (c) PBSG-005, (d) PBSG-010, (e) PBSG-030 and (f) PBSG-050 and the orientation degree of the PBS and its nanocomposites. (For interpretation of the references to colour in this figure legend, the reader is referred to the web version of this article.)

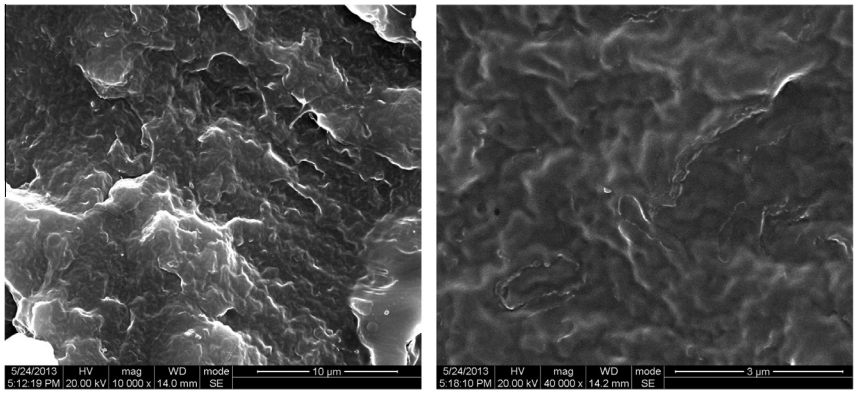

Fig. 10. SEM image of the PBSG-050 sample.

elongation at break reaches a platform. Besides, the tensile strength is decreased dramatically. This phenomenon may be caused by the agglomeration of GO in relative high loading samples and the reduction in orientation degree of these composite fibers. As well known, the orientation of polymer and fillers has a great effect on the mechanical performance of composites [38]. The 2D-WAXS technology was conducted to obtain necessary information for PBS matrix in the composite fibers. The 2D-WAXS patterns and the orientation degree of all samples are shown in Fig. 9. It has been demonstrated that the molecular orientation in the crystalline phase of composite fibers was decreased as the filler content increases. It means that the orientation of PBS can be obstructed by the graphene layers with relative rigidity property [39].

The dispersion of filler has an important influence on the performance of polymer composite. SEM was used to examine the quality of GO dispersion in these composites. However, as the content of GO is very low in this experiment, the GO sheets are difficult to observe. Thus, only preliminary results were presented in Fig. 10 and we will continue to search for a better characterization method. For SEM picture with low magnification (left), the content of GO is very low in this experiment, GO sheets could be barely found. In the relatively high magnification photographs (right), fuzzy interface between GO and PBS matrix can be observed, indicating a strong interfacial interaction between filler and the PBS matrix.

4. Conclusion

In this work, we fabricated PBS/GO composites through in-situ polymerization. GO sheets were thermo-reduced simultaneously to graphene during the reaction process and PBS chains were chemically grafted onto GO sheets by condensation reaction. The polymer-grafted GO showed good solubility in dichloromethane. This structure also endows GO sheets with a good compatibility and well dispersion in PBS matrix. We found that after excluding the influence of molecular weight, the performance of PBS can be evidently changed by introducing low content of GO into PBS matrix. The GO sheets can act as nucleating agent effectively to improve the crystallization rate of PBS. The hydrolytic degradation rate also can be improved eight times by only adding 0.1 wt% GO, and simultaneous enhancement in tensile strength and elongation of PBS can also be achieved by adding very low content of GO.

Acknowledgements

This work was supported by the National Natural Science Foundation of China (Grant No. 51173112 and Grant No. 51121001) and the Special Funds for Major State Basic Research Projects of China (2011CB606006).

References

[1] Zeng J-B, Li Y-D, Zhu Q-Y, Yang K-K, Wang X-L, Wang Y-Z. A novel biodegradable multiblock poly(ester urethane) containing poly(L-lactic acid) and poly(butylene succinate) blocks. Polymer 2009;50(5):1178–86.
[2] Xu J, Guo B-H. Poly(butylene succinate) and its copolymers: research, development and industrialization. Biotechnol J 2010;5(11):1149–63.
[3] Bi L, Wang J-W, Chen F, Fu Q. The effect of silica morphology on properties of PVA/silica nano-composites. Chin J Polym Sci 2013;31(11):1546–53.
[4] Nam TH, Goto K, Nakayama H, Oshima K, Premalal V, Shimamura Y, et al. Effects of stretching on mechanical properties of aligned multi-walled carbon nanotube/epoxy composites. Compos A 2014;64:194–202.
[5] Hong N, Zhan J, Wang X, Stec AA, Richard Hull T, Ge H, et al. Enhanced mechanical, thermal and flame retardant properties by combining graphene nanosheets and metal hydroxide nanorods for Acrylonitrile–Butadiene–Styrene copolymer composite. Compos A 2014;64:203–10.
[6] Wan Y-J, Gong L-X, Tang L-C, Wu L-B, Jiang J-X. Mechanical properties of epoxy composites filled with silane-functionalized graphene oxide. Compos A 2014;64:79–89.
[7] Lee C, Wei X, Kysar JW, Hone J. Measurement of the elastic properties and intrinsic strength of monolayer graphene. Science 2008;321(5887):385–8.
[8] Balandin AA, Ghosh S, Bao W, Calizo I, Teweldebrhan D, Miao F, et al. Superior thermal conductivity of single-layer graphene. Nano Lett 2008;8(3):902–7.
[9] Cai W, Zhu Y, Li X, Piner RD, Ruoff RS. Large area few-layer graphene/graphite films as transparent thin conducting electrodes. Appl Phys Lett 2009;95(12).
[10] Kim H, Macosko CW. Processing-property relationships of polycarbonate/graphene composites. Polymer 2009;50(15):3797–809.
[11] Zhang S-M, Zhang H-X, Zhang W-Y, Wu Z-Q, Chen F, Fu Q. Toughening of polycarbonate through reactive melt blending: effect of hydroxyl content and viscosity of hydroxyl-terminated polydimethysiloxane. Chin J Polym Sci 2014;32(7):823–33.
[12] Wang X, Yang H, Song L, Hu Y, Xing W, Lu H. Morphology, mechanical and thermal properties of graphene-reinforced poly(butylene succinate) nanocomposites. Compos Sci Technol 2011;72(1):1–6.
[13] Liu K, Chen L, Chen Y, Wu J, Zhang W, Chen F, et al. Preparation of polyester/reduced graphene oxide composites via in situ melt polycondensation and simultaneous thermo-reduction of graphene oxide. J Mater Chem 2011;21(24):8612–7.
[14] Wang XW, Zhang CA, Wang PL, Zhao J, Zhang W, Ji JH, et al. Enhanced performance of biodegradable poly(butylene succinate)/graphene oxide nanocomposites via in situ polymerization. Langmuir 2012;28(18):7091–5.
[15] Xu Z, Gao C. In situ polymerization approach to graphene-reinforced nylon-6 composites. Macromolecules 2010;43(16):6716–23.
[16] Solomon OF, Ciuta IZ. Determination of the intrinsic viscosity of polymer solutions by a simple determination of viscosity. J Appl Polym Sci 1962;6(24):683–6.
[17] Lee H-J, Oh S-J, Choi J-Y, Kim JW, Han J, Tan L-S, et al. In situ synthesis of poly(ethylene terephthalate) (PET) in ethylene glycol containing terephthalic acid and functionalized multiwalled carbon nanotubes (MWNTs) as an approach to MWNT/PET nanocomposites. Chem Mater 2005;17(20):5057–64.
[18] Tang Z, Kang H, Shen Z, Guo B, Zhang L, Jia D. Grafting of polyester onto graphene for electrically and thermally conductive composites. Macromolecules 2012;45(8):3444–51.
[19] Klein J. Repair or replacement–a joint perspective. Science 2009;323(5910):47–8.
[20] Lee SM, Cho D, Park WH, Lee SG, Han SO, Drzal LT. Novel silk/poly(butylene succinate) biocomposites: the effect of short fibre content on their mechanical and thermal properties. Compos Sci Technol 2005;65(3–4):647–57.
[21] Bourlinos AB, Gournis D, Petridis D, Szabó T, Szeri A, Dékány I. Graphite oxide: chemical reduction to graphite and surface modification with primary aliphatic amines and amino acids. Langmuir 2003;19(15):6050–5.
[22] Zhang H-B, Wang J-W, Yan Q, Zheng W-G, Chen C, Yu Z-Z. Vacuum-assisted synthesis of graphene from thermal exfoliation and reduction of graphite oxide. J Mater Chem 2011;21(14):5392–7.

[23] Stankovich S, Piner RD, Nguyen ST, Ruoff RS. Synthesis and exfoliation of isocyanate-treated graphene oxide nanoplatelets. Carbon 2006;44(15):3342–7.
[24] Kudin KN, Ozbas B, Schniepp HC, Prud'homme RK, Aksay IA, Car R. Raman spectra of graphite oxide and functionalized graphene sheets. Nano Lett 2007;8(1):36–41.
[25] Jin T-X, Zhou M, Hu S-D, Chen F, Fu Q, Fu Y. Effect of molecular weight on the properties of poly(butylene succinate). Chin J Polym Sci 2014;32(7):953–60.
[26] Yeh JT, Runt J. Multiple melting in annealed poly(butylene terephthalate). J Polym Sci Part B: Polym Phys 1989;27(7):1543–50.
[27] Tan S, Su A, Li W, Zhou E. New insight into melting and crystallization behavior in semicrystalline poly(ethylene terephthalate). J Polym Sci Part B: Polym Phys 2000;38(1):53–60.
[28] Todoki M, Kawaguchi T. Origin of double melting peaks in drawn nylon 6 yarns. J Polym Sci Part B: Polym Phys Ed 1977;15(6):1067–75.
[29] Shieh Y-T, Liu G-L. Temperature-modulated differential scanning calorimetry studies on the origin of double melting peaks in isothermally melt-crystallized poly(L-lactic acid). J Polym Sci Part B: Polym Phys 2007;45(4):466–74.
[30] Yasuniwa M, Satou T. Multiple melting behavior of poly(butylene succinate). I. Thermal analysis of melt-crystallized samples. J Polym Sci Part B: Polym Phys 2002;40(21):2411–20.
[31] Qiu Z, Ikehara T, Nishi T. Crystallization behaviour of biodegradable poly(ethylene succinate) from the amorphous state. Polymer 2003;44(18):5429–37.
[32] Alexis F. Factors affecting the degradation and drug-release mechanism of poly(lactic acid) and poly[(lactic acid)-co-(glycolic acid)]. Polym Int 2005;54(1):36–46.
[33] Pan H, Qiu Z. Biodegradable poly(L-lactide)/polyhedral oligomeric silsesquioxanes nanocomposites: enhanced crystallization, mechanical properties, and hydrolytic degradation. Macromolecules 2010;43(3):1499–506.
[34] Wang S, Han C, Bian J, Han L, Wang X, Dong L. Morphology, crystallization and enzymatic hydrolysis of poly(L-lactide) nucleated using layered metal phosphonates. Polym Int 2011;60(2):284–95.
[35] Cho K, Lee J, Kwon K. Hydrolytic degradation behavior of poly(butylene succinate) s with different crystalline morphologies. J Appl Polym Sci 2001;79(6):1025–33.
[36] Paul MA, Delcourt C, Alexandre M, Degée P, Monteverde F, Dubois P. Polylactide/montmorillonite nanocomposites: study of the hydrolytic degradation. Polym Degrad Stabil 2005;87(3):535–42.
[37] Vasanthan N, Ly O. Effect of microstructure on hydrolytic degradation studies of poly (L-lactic acid) by FTIR spectroscopy and differential scanning calorimetry. Polym Degrad Stabil 2009;94(9):1364–72.
[38] Murthy NS, Bray RG, Correale ST, Moore RAF. Drawing and annealing of nylon-6 fibres: studies of crystal growth, orientation of amorphous and crystalline domains and their influence on properties. Polymer 1995;36(20):3863–73.
[39] Dai X, Xu J, Guo X, Lu Y, Shen D, Zhao N, et al. Study on Structure and Orientation Action of Polyurethane Nanocomposites. Macromolecules 2004;37(15):5615–23.